

広島大学学術情報リポジトリ
Hiroshima University Institutional Repository

Title	Metamorphism on Wall Rocks of Some Bedded Cupriferous Pyritic Ore Deposits in the Sambagawa Metamorphic Zone
Author(s)	TAKEDA, Hideo
Citation	Geological report of the Hiroshima University , 12 : 361 - 379
Issue Date	1963-03-30
DOI	
Self DOI	10.15027/52540
URL	https://ir.lib.hiroshima-u.ac.jp/00052540
Right	
Relation	



Metamorphism on Wall Rocks of Some Bedded Cupriferous Pyritic Ore Deposits in the Sambagawa Metamorphic Zone

By

Hideo TAKEDA

with 3 Tables, 12 Text-figures, and 4 Plates

ABSTRACT: Those of the Shirataki and Sekizen mines situating near the Besshi mine in Central Shikoku are reasonably grouped into the bedded cupriferous pyritic ore deposit. The geological setting involved within the region of the Sambagawa crystalline schist consists mainly of the spotted epidote-hornblende schist and the spotted black schist accompanied with the spotted quartz schist together with the spotted sandy schist, all of which are probably corresponding to the epidote amphibolite facies in grade of metamorphism. Alteration of the related wall rocks has hitherto been believed to take place at the stage of ore formation nearly subsequent to completion of the regional metamorphism but is now, on the basis of fabric and chemical analyses, rather considered to have been related intimately to the regional metamorphism of its own.

CONTENTS

- I. Introduction
- II. Outline of Geology
- III. Ore Deposits
- IV. Metamorphism of Wall Rocks
- References

I. INTRODUCTION

It is well known that bulk of the bedded cupriferous pyritic ore deposits, such as those in Besshi, Sazare, Shirataki, Shingū, Kōtsu, Nonowaki, Chihara, Ōkuki, Iimori, Minenosawa and Kune, are found occurring in the Sambagawa crystalline schist region.

As for genesis of the deposits concerned, there have so far been various arguments combined with epigenetic hydrothermal origin by some authors or with syngenetic exhalation theory by others.

The epigenetic theory was advanced by KATŌ (1925), and has been supported by HORIKOSHI (1940), IMAI (1960) and so forth. HORIKOSHI concluded that the genesis of the deposits might have been related to the post activity of synkinematic basic intrusives, the sheared zones developed along the boundaries between quartz schist and other kind of rocks might have been provided for emplacement through ascending mineralizer, and the deposits were probably formed as a result of metasomatic replacement through hydrothermal solution filling the fissures nearly after recrystallization of the wall rocks.

The syngenetic theory was emphasized by KOJIMA and co-workers (1956), who

studied the stratigraphic situations of the deposits. According to their description, "the rise and fall in number of the deposits comprised in the stratigraphical succession of beds took place in a close relation to the activity of submarine volcanism at the geosyncline stage", and "the greater part of the deposits were formed of materials derived from the submarine eruption in the original geosyncline". WATANABE (1957) also supported the syngenetic theory in his investigation concerning genesis of the manganese deposits and the bedded ore deposits of cupriferous iron sulfide in Japan.

The confusion of argument seems to have been caused mainly by modification of the deposits due to the later regional metamorphism and by obliteration of almost all original features of the deposits.

In this study an attempt is made to define the metamorphism of wall rocks of some deposits comprised in the Shirataki and Sekizen mines. The deposits in question are considered to be suitable for clarifying the metamorphism because of their occurrence in an area revealing the highest grade of metamorphism in the Sambagawa metamorphic zone. For enlightening the stage of ore formation, it is of importance to determine whether the wall rocks might have been modified by regional metamorphism or not.

ACKNOWLEDGMENT: The writer wishes to express his sincere thanks to Professor Yoshio KINOSAKI of Hiroshima University for constant guidance in the course of this work. And sincere thanks are also due to Professor Takeo WATANABE of Tokyo University for his invaluable advices and encouragement. He is greatly indebted to Professor George KOJIMA and Lecturer Kei HIDE of Hiroshima University for their helpful suggestions and fruitful discussions. Heartly thanks are due to the geologists and mining engineers of Shirataki Mining Office of the Nippon Mining Co. Ltd. and of Besshi Mining Office of the Sumitomo Mining Co. Ltd. for assistance in carrying out his field work.

II. OUTLINE OF GEOLOGY

Geology of the Sambagawa crystalline schist region in Central Shikoku has been studied by many investigators since several decades ago, and KOJIMA and co-workers first established the stratigraphical succession as follows:

Yoshinogawa G*	{	Upper SG* Ojoin F*	{	Minawa upper M*
		Middle SG Minawa F		Minawa main green schist M
				Minawa lower M
Nishiiya G?	{	Lower SG {	Koboke F	
		Kawaguch F		
		Oboke F		

* G, SG, F, and M are abbreviations representing Group, Sub-group, Formation, and Member respectively.

The Lower and Upper sub-groups are predominant in black schist originated from argillaceous rock and in sandy schist derived from arenaceous rock, but the Middle sub-group consists mainly of green schists originated from the basic igneous rocks and pyroclastic rocks in connection with submarine volcanic activity at the geosyncline stage.

The Sambagawa metamorphic zone is divided into the spotted and the non-spotted sub-zones. The former is characterized by the rocks with albite porphyroblasts, but the latter by those without them. Roughly speaking, the grade of metamorphism in the spotted sub-zone is higher than that in the non-spotted sub-zone.

The monoclinical and isoclinal structures of steep folds are often found in the spotted sub-zone, while, on the contrary, the gentle folded structures are common in the non-spotted sub-zone.

In the Shirataki and Sekizen districts the geological setting composes mainly of the spotted epidote-hornblende schist and the spotted black schist accompanied with the spotted piedmontite-quartz schist or garnet-quartz schist and the spotted sandy schist. Many small lenticular masses of serpentinite are also found in the districts.

The main constituent minerals of the schists are as follows:

Spotted black schist: albite (porphyroblast)-quartz-muscovite-chlorite-graphite-granet-tourmaline-epidote-biotite-apatite-rutile-carbonate mineral (originated from argillaceous rock).

Spotted sandy schist: ditto (originated from arenaceous rock)*

Spotted quartz schist: albite (porphyroblast)-quartz-muscovite-chlorite-biotite-stilpnomelane-garnet-piedmontite-soda amphibole-epidote-rutile-carbonate mineral (originated from siliceous sediments).

Spotted epidote-hornblende schist: albite (porphyroblast)-common hornblende-chlorite-epidote-garnet-quartz-rutile-apatite-tourmaline-biotite-carbonate mineral (originated from basic igneous rocks and pyroclastic rocks).

In the districts, biotite and common hornblende together with garnet, muscovite, chlorite, and albite are included in the spotted black schist and spotted epidote-hornblende schist. Judging from these facts, the metamorphic facies of the schists seems to correspond to that of epidote amphibolite and, in other words, its grade of metamorphism may, according to the division given by MIYASHIRO and BANNO (1958), be equivalent to that in the transitional zone from Zone II to Zone III.

Stratigraphical horizon of the schists is situated in the Minawa upper formation, and the districts are structurally characterized by the recumbent anticlinal folding (Fig. 1).

* The mineralic constituents of the spotted sandy schist are same as those of the spotted black schist, but their texture and proportion of minerals contained differ from each other.

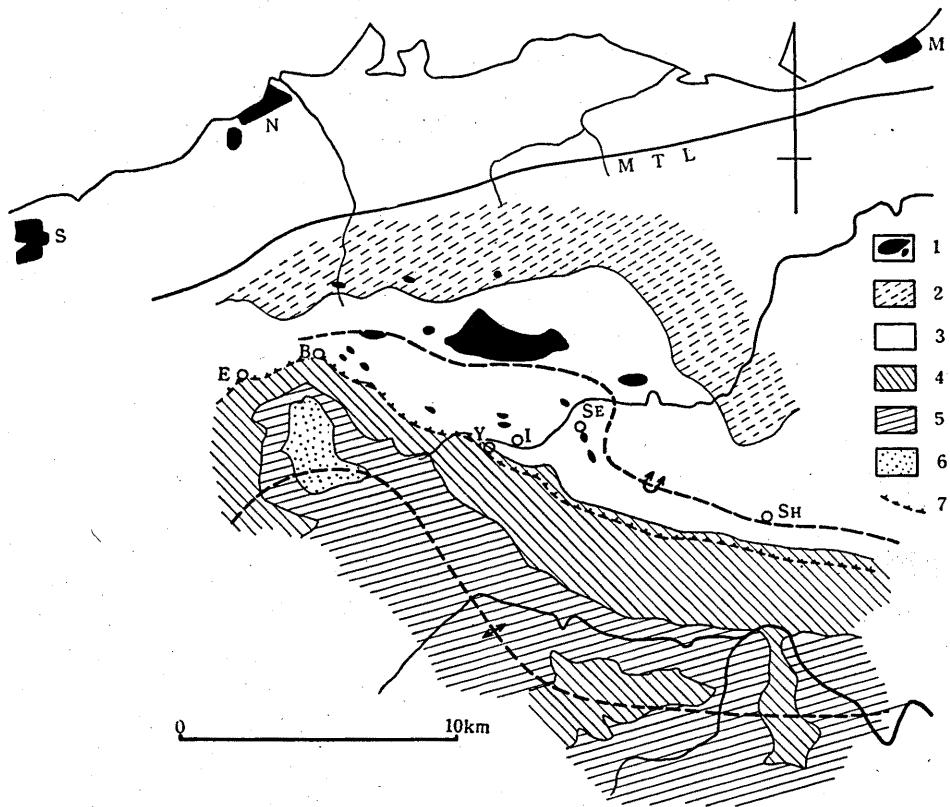


FIG. 1. Regional geological map showing the location of mines in the Besshi-Shirataki mining district. (After maps of K. HIDE and others.)

1. Ultrabasic rock.
2. Ōjōin formation.
3. Minawa upper member.
4. Minawa main green schist member.
5. Minawa lower member.
6. Koboke formation.
7. Boundary between non-spotted sub-zone and spotted sub-zone.

E-Ehime mine. B-Besshi mine. Y-Yokei mine. I-Ikadazu mine. SE-Sekizen mine. SH-Shirataki mine.

MTL-Median tectonic line.

S-Saijō city. N-Niihama city. M-Mishima city.

III. ORE DEPOSITS

The ore deposits of Shirataki and Sekizen mines are regarded as the bedded ones composing of cupriferous pyrite and grouped into the "Besshi-type deposit" called commonly in Japan or "Kieslager".

A. Main ore deposit of the Shirataki mine

The main ore deposit of the Shirataki mine, situating 17 km southeast of the Besshi mine, is known as one of the greatest deposits in the Sambagawa metamor-

phic zone. It is said that the mine was opened first in 1698 and the amount of smelted copper produced at that time was estimated 26 tons per month. After worked continuously with many interruptions until 1917, the ores with Cu content of 1.16% on an average, produced by the Nippon Mining Co. Ltd., were amount-ed to about 4,500,000 tons up to the present. The largest production in an year was about 230,000 tons in 1941. About 10,000 tons (per month) of the ores with 1.33% Cu and 14% S on an average are now being produced in the mine.

In the Shirataki mining district, there are several ore deposits named Upper Ōkawa, Lower Ōkawa, Kubo, Mominoki and Shimokawa exclusive of the Shirataki main ore deposit.

The main ore deposit under consideration is more than 4,000 m in the whole length along the plunge of asymmetrically overturned anticline and shows a remarkable continuity similar to in the case of other "Besshi type deposits". On the other hand, its extension along strike is variable in the range from 500 m to 800 m and its form is closely connected with the folded structure of wall rocks. In the western part of the deposit with gentle folded structure, its extension along strike is about 800 m and the thickness of ore bodies is invariable. In its eastern part with complicated structure of steep foldings, the extension along strike is about 500 m, and the thickness of ore bodies increases at the crest and the bottom of folding, but decreases on the wing, ranging from 0.3 m to 6 m in harmony with the folded structure (Fig. 2).

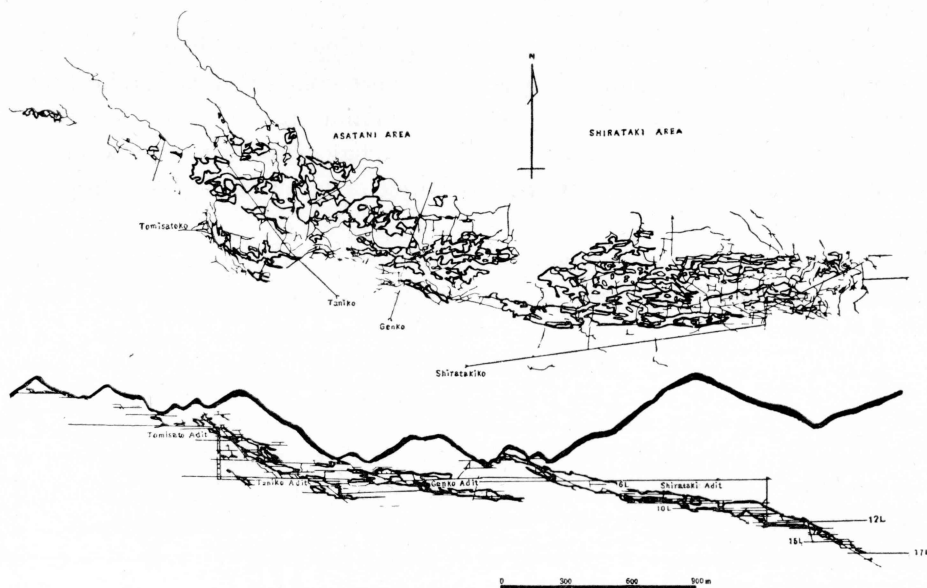


FIG. 2. Underground map (plan and section) of the Shirataki main ore deposit.

The main ore deposit is composed of several ore shoots found mostly along the axes of folded structure. Some are observable on the wing of gentle folding, but

none on the wing of steep folding. The ore shoots are variable in size and form, because they are nearly concordant with the folded structure of enclosing schists varying in trend along plunge. The length along their plunge varies from 100 m to 600 m, and that along their strike discloses a variation in the range from 20 m to 200 m.

Various kinds of ores revealing compact, banded, disseminated, and apophysis-like features as much as those rich in chalcopyrite are observed in the ore bodies.

The compact and banded ores are most abundant in the deposit, and compose mainly of pyrite associated with considerable amounts of chalcopyrite and sphalerite as well as small amount of bornite and chalcocite (Pl. 45, Fig. 2). In some parts of the banded ores included in the interior of ore bodies the intensely intraformational foldings are observed (Pl. 45, Fig. 1 and Pl. 47, Figs. 1 and 2).

The disseminated ores developed often along the marginal parts of compact pyritic ore bodies consist of disseminated pyrite crystals accompanied with considerable amounts of magnetite and hematite in wall rock, but sometimes are abundant in chalcopyrite and bornite. Chalcopyrite, sphalerite, quartz, chlorite and a carbonate mineral occur in the ores frequently as "pressure shadow" around crystals of pyrite and magnetite.

The ores rich in chalcopyrite are often found either within the compact ores or in their peripheries along strike-side. Main constituents of the ore are chalcopyrite, pyrite and sphalerite. These ores seem to have been originated through metamorphic differentiation of compact ores.

The apophysis-like ores are often observed branching perpendicular to the planer structure of wall rocks from the compact pyritic ore bodies and rich in bornite and chalcocite associated with small amounts of covellite, native silver, stromeyerite and some undetermined minerals. Bornite and chalcocite bear the microtextures indicating the intergrowth with triangular lattice or mutually intercalating one in the ore (Pl. 45, Fig. 3).

The gangue minerals accompanied in the ore are quartz, bluish soda-amphibole, chlorite, muscovite, albite, garnet, apatite and a carbonate mineral.

B. Sekizen ore deposit

The Sekizen mine, a branch of the Besshi mine, is located 7 km east of the latter, and has been worked by the Besshi Mining Office until 1958. Production of the ores with Cu content of 1.2% on an average in the mine was amounted to about 1,000 tons per month.

The deposit in this mine is constructed of several ore shoots with lenticular form in rather small scale: that is, the elongation of the deposit is about 100 m along strike-side, and the thickness of ore bodies is variable, because the ore bodies occur conformably with the structure of wall rocks revealing the intensely complicated folding (Fig. 3, Pl. 46, Fig. 1 and Pl. 47, Figs. 3 and 4).

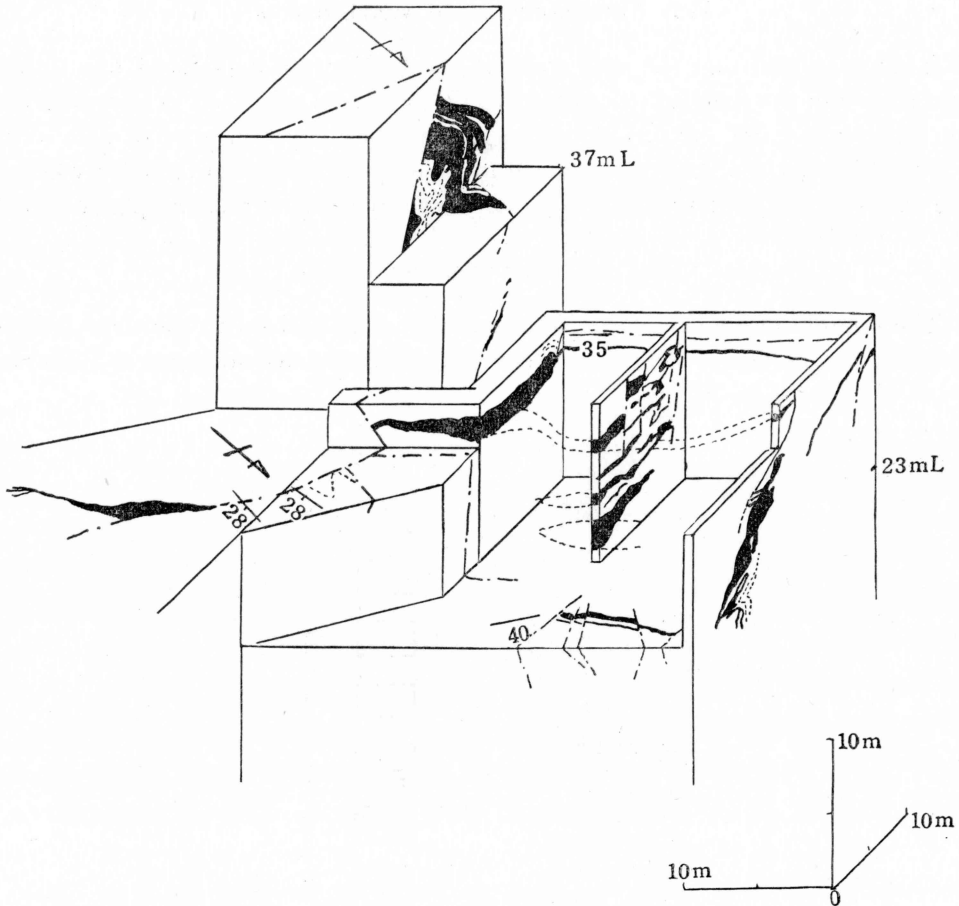


FIG. 3. Block diagram of Sekizen ore deposit. (After S. MORINAGA and others.)

The nature of the ores observed in this deposit is quite similar to that of the ores from the Shirataki main ore deposit. Intensely intraformational foldings are well observed in many parts of ore shoots, but pyrrhotite ores are often developed along the margins of compact pyritic ore bodies. In the pyrrhotite ore, oriented lamellar structure of pyrrhotite and valleriite with exsolved form in chalcopyrite grains are observed under the ore microscope (Pl. 46, Fig. 2).

The gangue minerals associated in the ores are also nearly same as those from the Shirataki main ore deposit excepting that biotite and stilpnomelane are often developed. Quartz and chlorite occur as "pressure shadow" around pyrite crystals (Pl. 46, Fig. 3).

Association of the lenticular ore bodies with the schistose serpentinites and actinolitic rocks is often observable and has so far been taken as a useful guide for pursuing the new ore bodies.

IV. METAMORPHISM OF WALL ROCKS

It has been said that the wall rocks of the bedded ore deposits of cupriferous iron sulfide in the Sambagawa metamorphic zone were subjected to hydrothermal alteration associating ore formation nearly after the recrystallization of wall rocks.

For clarifying the stage of ore deposition, it is interesting to consider whether the wall rocks might have been metamorphosed by regional metamorphism or not.

A. Shirataki main ore deposit

The stratigraphical succession of the ore-bearing horizon in the deposit is illustrated in Fig. 4, and the minerals constituting the related rocks are as follows:

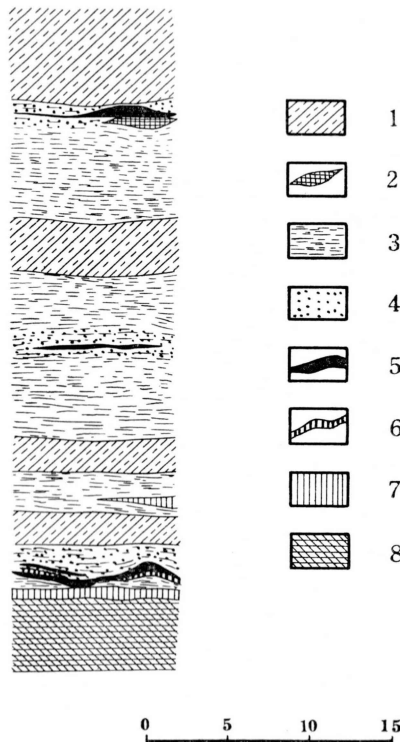


FIG. 4. Tentative column in the neighbourhood of ore-bearing horizon at Shirataki main ore deposit.

1. Spotted epidote-hornblende schist.
2. "Amphibolite".
3. "Phyllitic green schist".
4. Impregnated ore.
5. Massive ore.
6. Garnet-quartz schist.
7. Spotted muscovite-quartz schist.
8. Spotted black schist.

Spotted black schist: albite (porphyroblast)–quartz–muscovite–graphite–chlorite–tourmaline–garnet–epidote–apatite–biotite–carbonate mineral.

Spotted mica-quartz schist: quartz–albite (porphyroblast)–muscovite–chlorite–garnet–tourmaline–carbonate mineral.

Garnet-quartz schist: garnet-quartz-muscovite-bluish soda-amphibole-chlorite-epidote-carbonate mineral-magnetite-hematite.

“Amphibolite”*: bluish soda-amphibole-quartz-chlorite-carbonate mineral.

Spotted epidote-hornblende schist: albite(porphyroblast)-common hornblende-chlorite-epidote-muscovite-carbonate mineral-garnet-quartz-apatite-tourmaline-rutile-sphene-biotite-diopside.

“Phyllitic green schist in the impregnated sheared zone”: bluish soda-amphibole

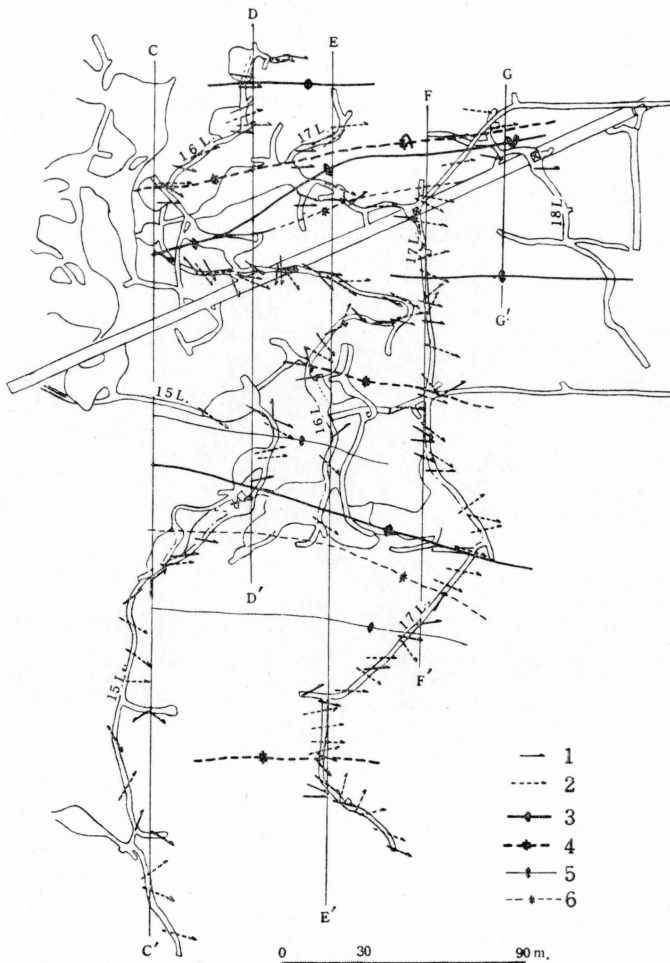


FIG. 5. Underground tectonic map showing the structures in the lower part of Shirataki pit.

1. Micro-corrugation axis.
2. Minor folding axis (β -axis).
3. Main anticline axis inclusive of isoclinal anticline axis.
4. Main syncline axis inclusive of isoclinal syncline axis.
5. Sub-anticlinal axis.
6. Sub-synclinal axis.

* The term of “amphibolite” here designates the monomineralic rock of bluish soda-amphibole.

–chlorite–epidote–albite(porphyroblast)–muscovite–quartz–apatite–rutile–sphene–garnet–carbonate mineral.

The “phyllitic green schist”* well developed around the pyritic ore bodies of Shirataki main ore deposit is megascopically dark green in color, remarkably schistose in texture, and often contains the disseminated crystals of pyrite and chalcopyrite. It has been considered that the schist was influenced by shearing movement and altered from spotted epidote-hornblende schist by hydrothermal solution at the stage of ore formation nearly after completion of the regional metamorphism.

The fabric analysis of planer and linear structures has been megascopically made by the writer as an attempt for inspecting the country rocks of the deposit. The scheme for studying the structures is essentially same as that described by SANDER (1948).

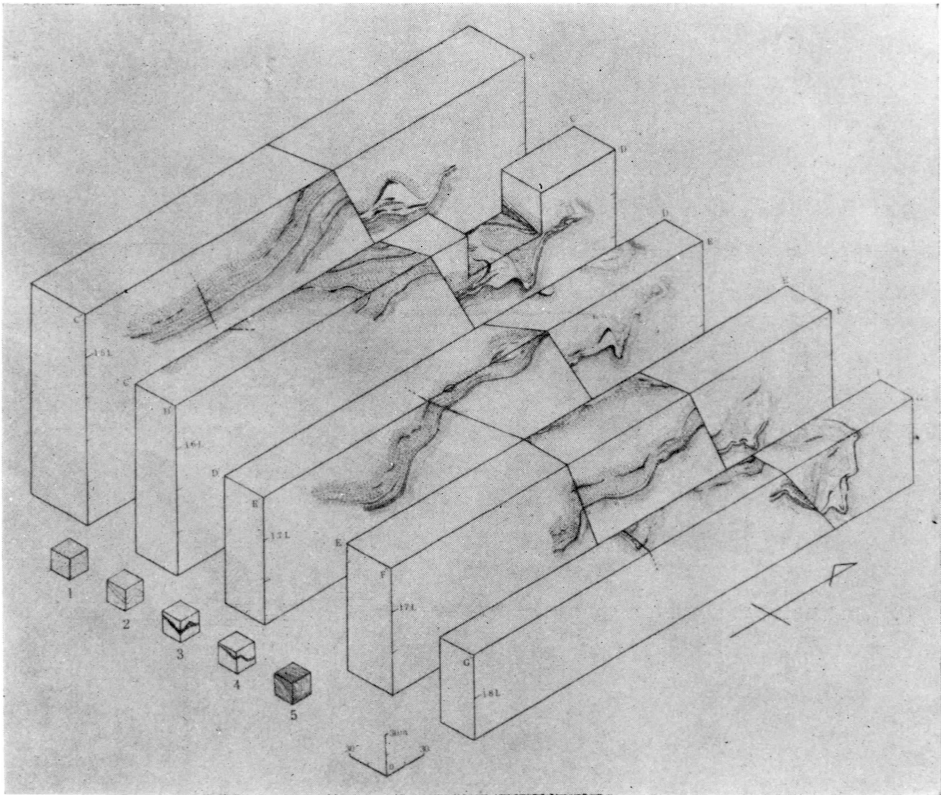


FIG. 6. Block diagram showing the complicated folded structure of the deposit in the part from 15th to 18th level of Shirataki pit.

1. Spotted epidote-hornblende schist. 2. “Phyllitic green schist”. 3. Ore body.
4. Spotted muscovite-quartz schist. 5. Spotted black schist.

* The “phyllitic green schist in the impregnated sheared zone” will hereunder be represented simply by “phyllitic green schist”.

For comparing the structures of the “phyllitic green schist” with those of other schists, π -diagrams for S_1 -plane obtained respectively on 15th, 16th, 17th and 18th levels in the pit of Shirataki mine are constructed, as are shown in Figs. 5 and 6. Poles of S_1 -planes of the spotted epidote-hornblende schist and spotted black schist are, because of the concordant structure of both schists, projected on an equiareal net given in Fig. 7a, while the π -diagram for S_1 -plane of “phyllitic green schist” is shown in Fig. 7b.

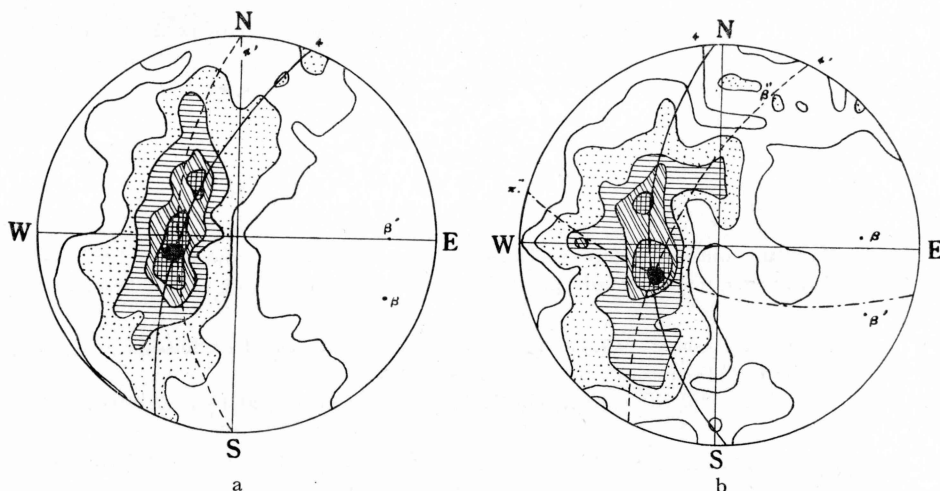


FIG. 7. π -diagrams for S_1 in the lower part of Shirataki pit.

- a. π -diagram of spotted black schist and spotted epidote-hornblende schist. 354 points. Contours: 8-7-5-3-1-0%.
- b. π -diagram of “phyllitic green schist”. 156 points. Contours: 9-7-5-3-1-0%.

The main girdle along great circle π around β (azimuth S 67° E, plunge 20°) and the sub-girdle along great circle π' around β' (azimuth E, plunge 25°) are found in Fig. 7a. On the contrary, two girdles along great circle π around β (azimuth N 86° E, plunge 30°), the great circle π' around β' (azimuth S 65° E, plunge 20°), and furthermore an imperfect girdle along the great circle π'' around β'' (azimuth N 13° E, plunge 20°) are illustrated in Fig. 7b.

As compared Fig. 7a with Fig. 7b, the main girdle and sub-girdle in Fig. 7a agree with the sub-girdle and main girdle in Fig. 7b respectively, and the imperfect girdle appears independently in Fig. 7b.

It should be considered that the π -diagrams are intimately related to the lineation diagrams of the schists, and accordingly the problems concerning π -diagrams will be discussed in connection with those of lineation diagrams.

An equal projection of the poles of lineation in the layers of spotted epidote-hornblende schist and spotted black schist, and those of “phyllitic green schist” are shown in Fig. 8. In Fig. 8a, N 84° E and 25° represent respectively the azimuth and plunge, the maximum of which indicates respectively East and 30° in Fig. 8b,

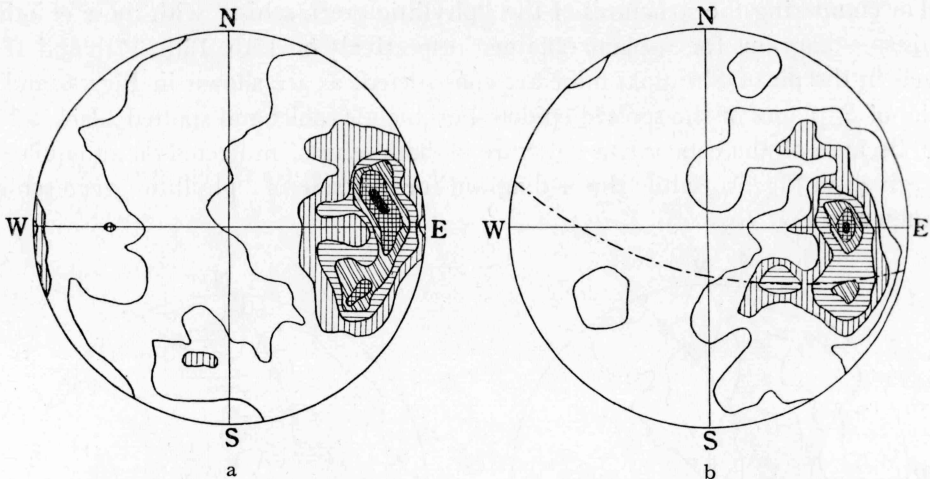


FIG. 8. Lineation diagram inclusive of β -axes of spotted black schist and spotted epidote-hornblende schist, and of "phyllitic green schist" in the lower part of Shirataki pit.

- a. Lineations and β -axes of spotted black schist and spotted epidote-hornblende schist. 142 points. Contours: 10-8-6-4-2-0%.
- b. Ditto of "phyllitic green schist". 62 points. Contours: 20-15-10-5-3-0%.

and another maximum, azimuth S 65° E and plunge 25°, is found in both diagrams, while the linear structures of the schists disclose imperfect girdles.

Besides, Fig. 8b reveals the presence of a maximum, azimuth S 38° E and plunge 55°, that is passed through by a great circle in Fig. 7b. It appears that the maximum is caused by bending movement when a competent body with lenticular form is sandwiched in an incompetent bed under stress condition and, on this occasion, the ore bodies seem to have played a role of the competent mass in the "phyllitic green schist".

In the lower part of the Shirataki pit, the main folding-axes have a tendency displaying divergency toward downstairs, and the structure shows a kind of deformed fan-shaped folding, while most of the lineations and β -axes bear the trends in harmony with the main folding-axes.

As are evident from the results of analysis of planer and linear structures, the π -diagrams for S_1 -plane have two girdles around rotation-axes with different trends, and should be closely connected with the maxima of the lineation diagrams. Comparing the π -diagram with the lineation diagram of "phyllitic green schist", the trends of main maximum and sub-maximum in the lineation diagram agree with those of the main rotation-axis and sub-rotation axis and, on the contrary, the trend of the main maximum in the lineation diagram of the spotted epidote-hornblende schist and spotted black schist is approximately in accordance with that of sub-rotation axis in the π -diagram of the schists, and the main rotation-axis in the π -diagram is coincident with that of sub-maximum in the lineation diagram, as are

Table 1. The trends of maximum in lincation diagrams and rotation axes in π -diagrams in the lower part of Shirataki pit.

Layer	L-diagram				π -diagram			
	main maxima		sub-maxima		main rotation axis		sub-rotation axis	
	azum.	plun.	azum.	plun.	azum.	plun.	azum.	plun.
Spotted black schist and spotted epidote-hornblende schist	N84°E	25°	S65°E	25°	S67°E	20°	E	25°
"Phyllitic green schist"	E	30°	S65°E	25°	N86°E	30°	S65°E	20°

shown in Table 1.

As for this case, two main interpretations concerning the relation between π -diagrams and lincation diagrams are possibly established.

First, the relation is happily maintained owing to numbers of localities and of measurements in the field work. Granting that the trends of structures are more important than the degree of concentration, it follows that three layers such as the spotted black schist, spotted epidote-hornblende schist and "phyllitic green schist" might have been resulted from simultaneous control by the same structural movement with two main trends of folding-axes, respective azimuth and plunge of which are N84°E~East, 25°~30° and S65~67°E, 20°~25°.

Second, the layers mentioned above were deformed at two main stages of folding during one cycle of kinematic movement. In the field, the S_1 -plane of the "phyllitic green schist" is found often oblique to that of the spotted epidote-hornblende schist at their boundary and mostly concordant with the boundary surface, whereas the S_1 -plane of the latter is discordant and rarely *vice versa* (Fig. 9).

On the other hand, the S_1 -plane of the former seems to have been deformed later in stage than that of the latter. Accepting this view, the stage prior to that of folding movement may be represented by the main girdle along the great circle π around β in Fig. 7a, and the main girdle π around β in Fig. 7b may correspond to the later stage.

It is possible to suppose that the trend of the main fold-axis varied from S65°~67°E to E~N84°E in azimuth and from 20°~25° to 25°~30° in plunge through kinematic movement, and all layers were controlled by the prior and later movements, but the structures of the spotted black schist and spotted epidote-hornblende schist were mainly formed by the prior kinematic movement, while those of the "phyllitic green schist" were constructed by the later movement.

Under the microscope, the main constituents of the "phyllitic green schist" are bluish soda-amphibole, albite porphyroblast, chlorite, muscovite, epidote, and quartz, among which the first and the third seem to have been in an equilibrate relation during regional metamorphism, because chloritization and other hydro-

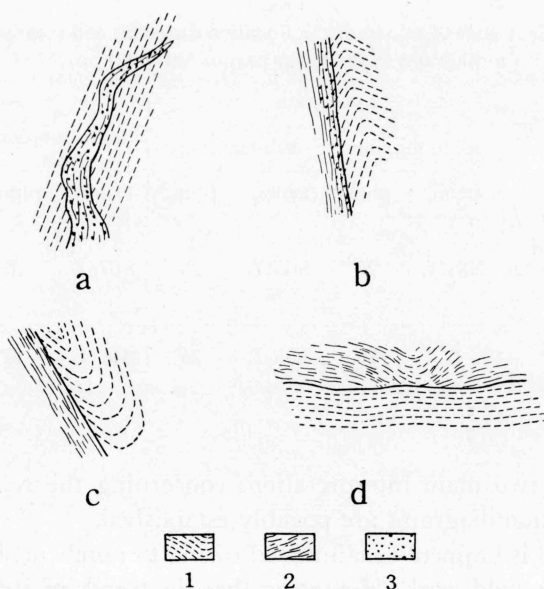


FIG. 9. Sketch showing the relation of S_1 -planes between spotted epidote-hornblende schist and "phyllitic green schist" in the 10th level of Shirataki pit.

1. Spotted epidote-hornblende schist. 2. "Phyllitic green schist". 3. Impregnated ore.

thermal alteration of metamorphic mineral could not be observed in the schist (Pl. 48, Fig. 1, 2).

The proportion of these constituent minerals is not constant: that is, some parts compose mainly of soda-amphibole, epidote, chlorite, quartz, and muscovite associated with small amounts of albite porphyroblast, and other parts, of albite porphyroblast, chlorite, soda-amphibole and epidote. Roughly speaking, the schist with more amounts of albite porphyroblast contains less amounts of soda-amphibole, and *vice versa*.

For comparing chemical property and mineral assemblage of the spotted epidote-hornblende schist with those of the "phyllitic green schist", chemical and modal compositions of the related schists are shown in Table 2, and ACF diagram is given in Fig. 10.

As are conspicuous in Table 2, the spotted epidote-hornblende schists are comparatively abundant in CaO, while the "phyllitic green schists" are rather rich in H_2O , Al_2O_3 and TiO_2 . Both schists are not so much variable in Na and K contents and poor in SiO_2 on the whole. MgO is not so much abundant in the latter.

In case of the latter, variation is observable not so much in the bulk chemical composition but in the modal composition.

It is interesting that the chemical composition $Na_2O + K_2O$ fulfilled with alkali amphibole in the schist is similar to that predominant in albite porphyroblast.

Table 2. Chemical and modal compositions of spotted epidote-hornblende schist and "phyllitic green schist".

	1	2	3	4	5	6	7
SiO ₂	47.78	46.64	43.46	48.86	47.10	43.33	45.80
TiO ₂	0.19	0.09	0.16	1.05	0.17	0.24	0.23
Al ₂ O ₃	16.50	15.99	15.79	17.80	17.38	17.41	18.90
FeO	7.90	4.71	4.13	7.39	7.98	6.53	5.76
Fe ₂ O ₃	4.87	4.67	6.84	4.87	3.48	4.30	5.77
MnO	0.16	0.11	0.21		0.14	0.14	0.18
MgO	6.48	7.66	6.32	3.87	7.55	10.39	5.84
CaO	10.42	12.99	12.14	10.50	9.05	8.92	8.07
Na ₂ O	2.79	2.42	2.81	2.32	2.61	2.04	3.20
K ₂ O	0.05	0.22	0.66	0.86	0.65	0.66	1.26
P ₂ O ₅	0.03	0.00	0.07	0.60	0.00	0.06	0.09
Cr ₂ O ₃	0.03	0.66	0.33		0.02	0.17	0.15
H ₂ O (+)	1.51	1.52	1.35	1.29	2.06	3.61	2.54
H ₂ O (-)	0.32	0.32	0.32		0.28	0.48	0.38
CO ₂				0.65			
Ig. loss*	2.02	3.30	6.60	1.94	3.56	5.30	4.16
Total	99.12	99.46	99.52	100.44	99.69	99.60	99.47
Hornblende	17.8	47.2	35.5				
Soda amphibole					54.8	21.7	16.8
Albite	22.5	20.3	23.6		1.4	27.0	3.4
Epidote	24.2	19.0	19.9		24.3	9.4	35.2
Chlorite	2.1	4.7	3.1		8.9	32.3	13.1
Muscovite	24.0	1.5	9.5		3.8	2.4	20.5
Quartz	4.8	2.6	1.4		5.9	1.1	1.7
Sphene	1.0				2.1	4.2	6.9
Rutile	0.7	0.2	1.6		1.2		1.7
Carbonate	1.4	4.5	7.5			0.2	
Ore mineral	1.4		2.0		0.2		
1.	Spotted epidote-hornblende schist (HT. 55080605). Anal. by M. KAWANO.						
2.	Ditto (HT. 55072701). Ditto.						
3.	Ditto (HT. 55050911). Ditto.						
4.**	Ditto. Anal. by J. SUZUKI.						
5.	"Phyllitic green schist" (HT. 55050403). Anal. by M. KAWANO.						
6.	Ditto (HT. 55080302). Ditto.						
7.	Ditto (HT. 55050507). Ditto.						

* In the ignition loss small amounts of CO₂ and S are included besides H₂O.

** Reported by J. SUZUKI in 1930.

Judging from the chemical and petrographical characters, the metamorphism recognized in the "phyllitic green schists" seems to bear a resemblance to that in

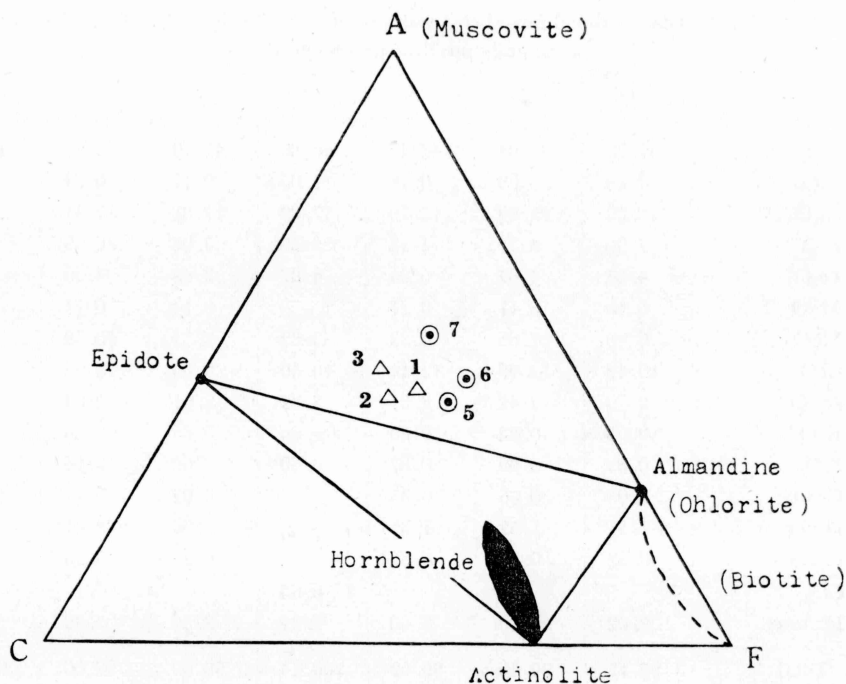


FIG. 10. ACF diagram of spotted epidote-hornblende schists and "phyllitic green schists".

the glaucophane schist, and is considered to have been developed under high-pressure and low-temperature conditions.

Furthermore, a small lenticular mass of the light green-colored schist is sometimes found in the "phyllitic green schist". Under the microscope, the massive schist composes mainly of albite porphyroblast, muscovite, chlorite, garnet and quartz associated with small amounts of common hornblende. Albite porphyroblasts contain the inclusions composing mostly of garnet, and some of their crystals are distorted and show conspicuously undulatory extinction. Quartz grains are minute in size in some parts abundant in muscovite. On the other hand, the inclusions of albite porphyroblast without undulatory extinction in the spotted epidote-hornblende schist consist of epidote, quartz, muscovite and hornblende (Pl. 48, Fig. 3).

It seems that the lenticular mass of the green schist is a sort of phyllonite originated from the spotted epidote-hornblende schist under sheared condition.

As the results of fabric and chemical analyses, the "phyllitic green schist" including the ore bodies is deduced to have been metamorphosed through the same metamorphic process as that for other schist and, however, to have been subjected to higher stress than that for other schists.

B. Sekizen ore deposit

The relation between the ore bodies and the wall rocks in the Sekizen ore de-

posit is illustrated in Figs. 11 and 12. As the wall rocks, the spotted black schist associated with the garnet-quartz schist, spotted green schist and spotted epidote-hornblende schist are mainly observable. The bulk constituents of the schists are as follows:

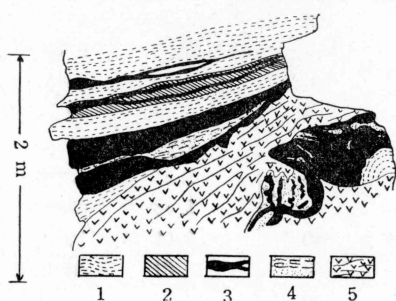


FIG. 11. Sketch showing the relation between ore bodies and wall rocks. (After S. MORINAGA and others)

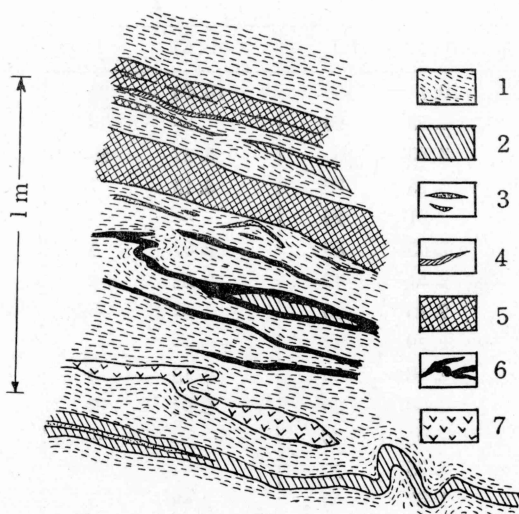


FIG. 12. Sketch showing the relation between ore bodies and wall rocks.

Spotted black schist: albite (porphyroblast)-biotite-muscovite-garnet-quartz-tourmaline-apatite-rutile-carbonate mineral.

Garnet-quartz schist: garnet-quartz-muscovite-albite (porphyroblast)-chlorite-biotite-stilpnomelane-soda amphibole-tourmaline-rutile-carbonate mineral.

Spotted green schist: albite (porphyroblast)-muscovite-actinolite-chlorite-epidote-quartz-sphene-carbonate mineral.

Spotted epidote-hornblende schist: albite (porphyroblast)-muscovite-epidote-common hornblende-chlorite-quartz-rutile-carbonate mineral.

Besides, the lenticular masses of the schistose serpentinites and actinolitic rocks are often found near the ore bodies in the deposits.

Spotted black schist and garnet-quartz schist are predominant in biotite near by the boundary between the ore bodies and the wall rocks. Seam-like occurrence of biotite is sometimes observable along the similar boundary (Fig. 11), and albite veinlets are often found in the wall rock.

Under the microscope, the biotite crystals around the ore minerals are not replaced by chlorite and muscovite, and soda-amphibole crystals are arranged along the boundary of ores. The metamorphic minerals are considered to have not been hydrothermally altered and to have been formed in equilibrium relation with hydrous and ore minerals during the regional metamorphism (Pl. 48, Figs. 4 and 5).

Biotite, soda-amphibole and stilpnomelane occurring also as gangue minerals in

the deposit have been identified after separation by means of the isodynamic separator through X-ray powder method (Table 3).

Table 3. X-ray Powder Data of Biotite and Stilpnomelane from Sekizen Mine

1		2		3		4	
d (Å)	I/I ₀	d (Å)	I	d (Å)	I/I ₀	d (Å)	I
10.1	100	10.03	85	11.9	100	12.2	45
4.58	20	—	—	—	—	10.03	67*
3.36	100	3.37	58	—	—	8.50	33**
3.15	20	3.18	7	—	—	6.14	2
2.91	20	—	—	4.04	50	4.03	10
2.65	80	2.62	5	—	—	3.37	52*
2.51	40	2.52	9	—	—	3.13	68**
2.45	80	—	—	3.03	40	3.02	10
2.28	20	—	—	—	—	2.81	8
2.18	80	2.18	5	2.70	20	—	—
2.00	80	2.02	10	2.56	40	2.59	9
1.91	20	—	—	2.34	30	—	—
1.75	20	—	—	—	—	2.18	15*
1.67	80	1.68	5	2.11	20	—	—
1.54	80 S	1.54	4	—	—	2.01	8*
1.47	20	—	—	—	—	1.68	5*
1.43	20	—	—	1.58	30	—	—
1.36	60	1.37	4	1.56	30	—	—
1.33	40	—	—	1.52	20	—	—
1.31	40	—	—	—	—	—	—
Biotite				Stilpnomelane			
1. Biotite from Edenville, U. S. A.				3. Stilpnomelane from Genoa Mine			
2. Biotite from Sekizen Mine				4. Stilpnomelane from Sekizen Mine			

* biotite

** amphibole

The optical inspection of stilpnomelane indicates that most of its crystals are ferric ones, but some are ferrous ones in kind.

The paragenesis of biotite with stilpnomelane and that of stilpnomelane with pyrite were reported by Hutton (1938) who suggested that the latter relation might have been originated in bog-iron ore.

It appears that the occurrence of the stilpnomelane so far found by the writer as gangue mineral in many bedded cupriferous pyritic ore deposits in the Sambagawa metamorphic zone is closely connected with the genesis of the deposits.

In view of the above-mentioned results, the writer finds it difficult to avoid the conclusion that the wall rocks of Shirataki main ore deposit and Sekizen ore deposit were later modified by regional metamorphism, and some wall rocks, such as "phyllitic green schist", were derived from hydrothermally altered rocks associating ore formation at a prekinematic stage.

REFERENCES

- FYFE, W. S., TURNER, F. J. and VERHOOGEN, J. (1958): Metamorphic reactions and metamorphic facies. *Geol. Soc. Amer., Mem.* 73.
- HIDE, K. (1954): Geologic structure of the Shirataki mining district, Kochi prefecture (in Japanese). *Geol. Rept. Hiroshima Univ.*, (4), 47~83.
- HIDE, K., YOSHINO, G. and KOJIMA, G. (1956): Preliminary report on the geologic structure of the Besshi spotted schist zone (in Japanese). *Jour. Geol. Soc. Japan*, 62, (733), 574~584.
- HORIKOSHI, Y. (1940): Morphological studies of the Besshi type ore deposits (in Japanese). *Rept. 2, 2nd sub-Com., Japan Soc. for the promotion of Sci.*, (1), 1~23.
- HUTTON, C. O. (1938): The stilpnomelane group of minerals. *Min. Mag.*, 25, (163), 172~206.
- IMAI, H. (1960): Geology of the Okuki mine and other related cupriferous pyrite deposits in the southwestern Japan. *N. Jb. Min. Abh.*, 94, 352~389.
- KATO, T. (1925): The problems of the cupriferous pyritic deposits. *Econ. Geol.*, 20, (1), 97~100.
- KOJIMA, G., HIDE, K. and YOSHINO, G. (1956): The stratigraphical position of Kieslager in the Sambagawa crystalline schist zone in Shikoku (in Japanese). *Jour. Geol. Soc. Japan*, 62, (724), 30~45.
- MIYASHIRO, A. and BANNO, S. (1958): Nature of glaucophanitic metamorphism. *Amer. Jour. Sci.*, 256, 97~110.
- MORINAGA, S., KANAOKA, T. and KONDO, K. (1955): Besshi mine. Ore deposits and geologic structure (II) (in Japanese). *Technical texts of Japan Mining Assoc.*, (11), 65~73.
- SANDER, B. (1946): Einführung in die Gefügekunde der geologischen Körper. I, II, Wien u. Innsbruck.
- SUGIYAMA, R. (1955): Linear structure of the country rocks of the "Kieslager", and "L-S fabric analysis" (in Japanese), *Jour. Sci. Rept. Niigata Univ.*, 2, 3, (1), 1~66.
- SUZUKI, J. (1930): Petrological study of the crystalline schist of Shikoku, Japan. *Jour. Fac. Sci. Hokkaido Univ.*, 4, (2), 27~107.
- TAKEDA, H. (1960): Geology and ore deposits of the Shirataki mine, Kochi prefecture (in Japanese). *Mining Geol.*, 10, (40), 85~93 and (41), 127~140.
- TAKEDA, H. and SEKINE, Y. (1960): A consideration on the metamorphism of cupriferous pyritic deposit at Sekizen, Ehime prefecture (in Japanese). *Mining Geol.*, 10, 44, 369~379.
- WATANABE, T. (1957): Genesis of bedded manganese deposits and cupriferous pyrite deposits in Japan (in Japanese). *Mining Geol.*, 7, (24), 87~97.
- ZAVARITSKY, A. N. (1950): Metasomatism and metamorphism in the pyrite deposits of the Urals. *Int. Geol. Congr., Rept. 18th Ses., Pt. III, Proc. Sec. B., Metasomatic process in metamorphism.*



EXPLANATION OF PLATE XLV

- FIG. 1. Intraformational folding with metasomatic replacement of chalcopyrite rich ore in the interior of ore body at 19th level in the Shirataki pit.
- FIG. 2. Photograph of compact ore (HT. 55072803). Section parallel to ac-plane. $\times 40$.
py—pyrite. sl—sphalerite. G—gangue mineral.
- FIG. 3. Photomicrograph of triangular lattice intergrowth of bornite and chalcocite (HT. 56080203). Under the oil immersion lens. $\times 400$.
Gray part—bornite. White part—chalcocite.

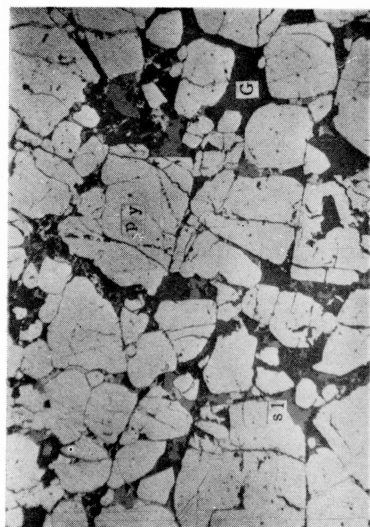


FIG. 2.

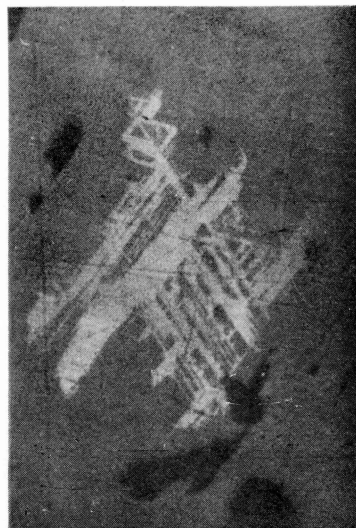


FIG. 3.



FIG. 1.

EXPLANATION OF PLATE XLVI

- FIG. 1. Intraformational folding of ore body at Sekizen deposit.
- FIG. 2. Photomicrograph of valleriite in chalcopyrite. Under the oil immersion lens. $\times 500$.
va—valleriite. cp—chalcopyrite.
- FIG. 3. Photomicrograph of "pressure shadow" of quartz around pyrite crystals. Crossed nicols.
 $\times 40$.
py—pyrite. qz—quartz.

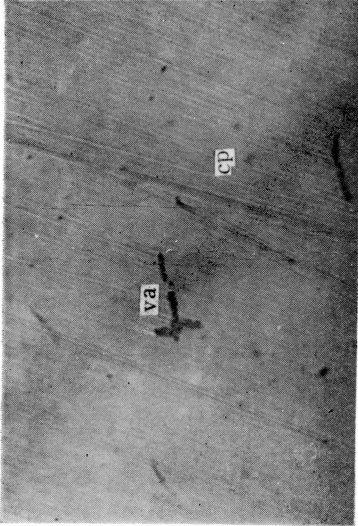


FIG. 2.

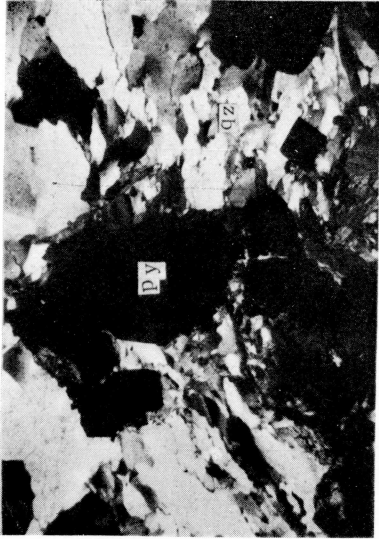


FIG. 3.



FIG. 1

EXPLANATION OF PLATE XLVII

- FIG. 1. Folded structure of pyritic ore from Shirataki main ore deposit. Polished surface of hand specimen normal to b-axis.
Sketch showing ditto: white part-pyritic ore, black part-gangues, oblique line part-chalcopyrite rich ore.
- FIG. 2. Ditto.
- FIG. 3. Folded structure of pyritic ore with pyrrhotite veinlet from Sekizen deposit. Polished surface normal to b-axis.
Sketch showing ditto: oblique line part-ore, black part-pyrrhotite veinlet (po), white part-gangues.
- FIG. 4. Ditto.
Sketch showing ditto: ORE-pyritic ore, mt-magnetite, po-pyrrhotite.



FIG. 1.

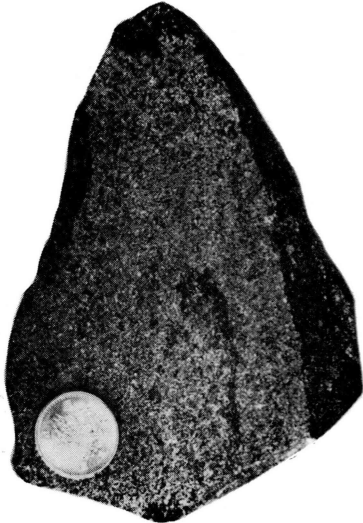


FIG. 2.

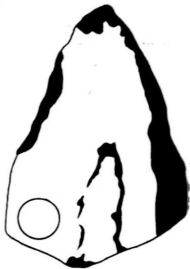


FIG. 3.

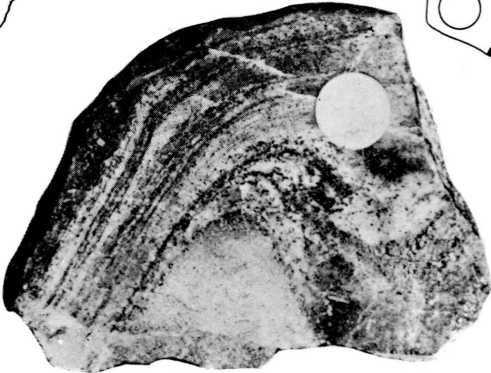
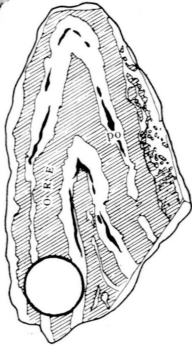
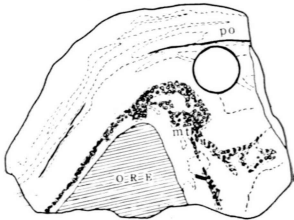


FIG. 4.



EXPLANATION OF PLATE XLVIII

Photomicrographs.

- FIG. 1. "Phyllitic green schist" with folded structure from Shirataki main ore deposit. Section normal to b-axis. One nicol. $\times 40$.
sa—soda amphibole. Q—quartz.
- FIG. 2. Boundary between pyritic ore and "phyllitic green schist" from Shirataki main ore deposit. One nicol only. $\times 55$.
sa—soda amphibole. py—pyrite.
- FIG. 3. Phyllonite in the "phyllitic green schist". Crossed nicols. $\times 50$.
ab—albite porphyroblast. Q—quartz.
- FIG. 4. Biotite around pyrite crystals at the boundary between pyritic ore and wall rock from Sekizen deposit. One nicol. $\times 40$.
bio—biotite. gar—garnet. py—pyrite.
- FIG. 5. Soda amphibole around pyritic ore from Sekizen ore deposit. One nicol. $\times 40$.
sa—soda amphibole. py—pyritic ore.

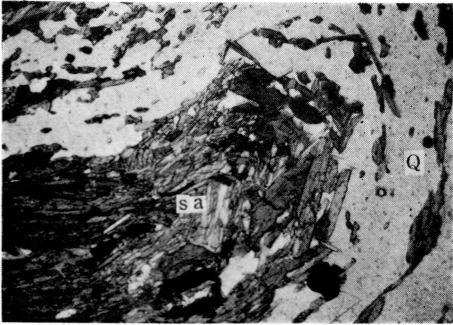


FIG. 1.

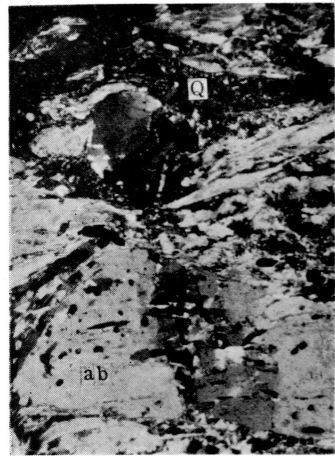


FIG. 3.

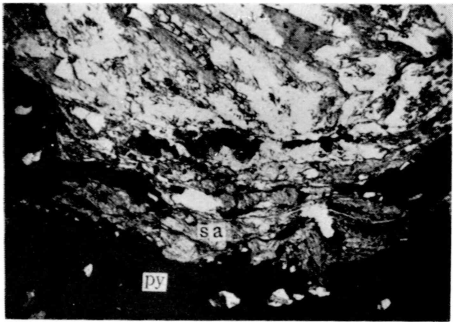


FIG. 2.

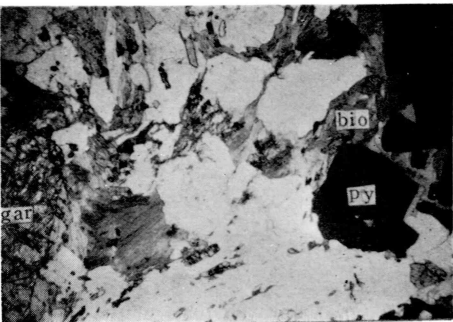


FIG. 4.

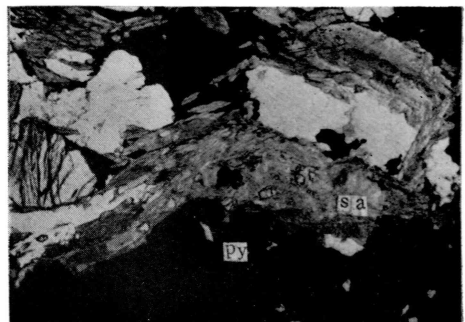


FIG. 5.